Conductance of α-Helical Peptides Trapped within Molecular Junctions

Slawomir Sek,* Aleksandra Misicka, Karolina Swiatek, and Elwira Maicka

Department of Chemistry, University of Warsaw, Pasteura 1, 02093 Warsaw, Poland

Received: May 19, 2006; In Final Form: July 14, 2006

Self-assembled monolayers of α-helical peptides on a gold surface were employed as model systems for the investigation of mediated electron transfer. The peptides contained 14, 15, 16, and 17 amino acid residues. The measurements of electron transmission through single molecules of helical peptides were performed using scanning tunneling spectroscopy (STS). The molecules were trapped between the gold tip and the substrate. Electrical contact between the molecule and the gold probe was achieved by the use of peptides containing thiol groups present at each end of the helix. The conductance behavior of the peptides was examined as a function of tip−substrate distance at fixed bias voltage. Measurements performed with peptides containing different numbers of amino acid residues indicate that the distance dependence of electron transmission through an α-helix is weaker than that through simple *n*-alkyl bridges.

Introduction

The importance of peptides in mediating electron transfer in biological systems is unquestionable.[1−3] However, the exact mechanism of this process is still controversial. It has been shown in numerous reports that two mechanisms can contribute to electron transfer through peptides: superexchange and hopping.[4−10] Theoretical considerations as well as some experimental studies indicate that the first mechanism is valid for short-chain peptides whereas the second contributes significantly to electron transfer for longer spacers.[4,6] The distinction between these two mechanisms can be made on the basis of the distance dependence of electron transfer. Considering the change of an arbitrarily chosen parameter related to the rate of electron transport as a function of the length of the molecular bridge, the dependence is expected to be exponential for the superexchange mechanism and linear for hopping.[4,10,11] Thus, the distance dependence in the case of the hopping mechanism is much weaker than that for superexchange tunneling. Such a model seems to explain efficient electron-transfer mediation observed for long amino acid sequences.[5,9,12] Moreover, a transition between the superexchange and hopping mechanisms was experimentally observed for oligoprolines.[6] Unfortunately, the conclusions from studies on particular bridges cannot be generalized for all systems because a number of factors other than the length of the spacer influence the overall electron transfer through peptides. These include the details of the amino acid sequence, the secondary structure of the peptide, and the presence of hydrogen bonds. For example, upon comparison of the electrochemical data obtained for α-helical peptides, it is evident that the rate constants of electron transfer vary significantly although the lengths of the spacers are similar.[5,9] This probably reflects the differences in the details of amino acid sequences. Several groups have also demonstrated the influence of the secondary structure of the peptide on electron-transfer efficiency.[13−17] Shin and co-workers showed in their theoretical study that the parameter that describes the ability of the bridge to mediate the electron transfer, i.e., the distance decay constant (β), is sensitive to the secondary structure of the peptide backbone in the case of the superexchange mechanism.[13] Ghiggino and co-workers observed the different distance dependences for photoinduced electron transfer through α-helical and β-sheet structures and found corresponding decay constants of 0.66 and 0.73 $Å^{-1}$, respectively.[14,15] A very weak distance dependence for 3_{10}-helices of aminoisobutyric oligomers was reported by Maran and co-workers, who attributed this result to the effect of intramolecular hydrogen bonding on the electron-transfer rate.[16] Kraatz and co-workers also observed a shallow distance dependence of the electron-transfer rate for collagen-like peptide assemblies with interstrand hydrogen bonds.[17] All of these results clearly show that the variability in electron-transfer efficiency for peptide bridges is related to a number of factors that control the structures of the individual peptide backbones as well as the larger peptide assemblies.

We believe that the present work will contribute to the understanding of the mechanism of electron transfer through peptide bridges. We report here conductance measurements of single α-helical peptide molecules with different lengths. The efficiency of electron transmission through the peptides was investigated using the scanning-tunneling-microscopy- (STM-) based molecular junction method, which involves the entrapment of single molecules between the STM tip and the substrate. This approach has been successfully utilized for conductance measurements of dithioderivatives of alkanes, carotenoid polyenes, DNA, viologen, and short-chain peptides consisting of 2−4 amino acid residues.[18−26] In this article, we describe molecular junction experiments performed with monolayers of α-helical peptides containing 14−17 amino acid residues. Because the peptides are asymmetric, we used a monolayer preparation procedure leading to the uniform orientation of molecules on the surface. Previously, it was shown that molecular junctions formed with α-helical peptides produce asymmetric current−voltage responses; thus, control of the orientation of the molecules is crucial to obtain reproducible results.[27] The efficiency of electron transmission through peptides was compared to that through *n*-alkanedithiols.

* To whom correspondence should be addressed. E-mail: slasek@chem.uw.edu.pl.

10.1021/jp063073z CCC: $33.50
Published on Web 09/12/2006

CHART 1: Chemical Structures of the α-Helical Peptides

P14AA:
Cys(S-Acm)-Ala-Lys-(Glu-Ala-Ala-Ala-Lys)$_2$-Ala-NH-(CH$_2$)$_2$-SH

P15AA:
Cys(S-Acm)-Ala-Ala-Lys-(Glu-Ala-Ala-Ala-Lys)$_2$-Ala-NH-(CH$_2$)$_2$-SH

P16AA:
Cys(S-Acm)-Ala-Ala-Ala-Lys-(Glu-Ala-Ala-Ala-Lys)$_2$-Ala-NH-(CH$_2$)$_2$-SH

P17AA:
Cys(S-Acm)-Glu-Ala-Ala-Ala-Lys-(Glu-Ala-Ala-Ala-Lys)$_2$-Ala-NH-(CH$_2$)$_2$-SH

Ala = alanine
Lys = lysine
Glu = glutamic acid
Acm = acetamidomethyl

Experimental Section

All chemicals and starting materials for syntheses were purchased from Sigma, Aldrich, Novabiochem, and POCh Gliwice. The synthesis of the peptides was performed manually by solid-phase techniques starting from cysteamine 4-methoxytrityl resin. We synthesized peptides built of 14 (P14AA), 15 (P15AA), 16 (P16AA), and 17 (P17AA) amino acid residues. Each peptide contained a cysteamine linker at the C-terminus and a cysteine (Cys) at the N-terminus. The thiol group of cysteine was protected with an acetamidomethyl group (Acm), which was removed after the deposition of the peptide on the gold surface.[27,28] The detailed amino acid sequences of the peptides are shown in Chart 1. The final products were purified by reverse-phase high-performance liquid chromatography (RP-HPLC) and analyzed by mass spectrometry. ESI MS: P14AA, $[M + 3H]^{3+}$ $m/z = 488.2$; P15AA, $[M + 2H]^{2+}$ $m/z = 767.1$; P16AA, $[M + 2H]^{2+}$ $m/z = 802.6$; P17AA, $[M + 2H]^{2+}$ $m/z = 867.8$. The amino acid sequences in the peptides were chosen as helix-favoring. The helicity of the peptides was confirmed by circular dichroism (CD) measurements. In all cases, the CD spectra exhibited a double-minimum pattern at 208 and 222 nm, which is characteristic of α-helical conformation. 1,10-Decanedithiol and 1,12-dodecanedithiol were synthesized in a reaction between dibromoalkyls and thiourea and subsequent basic hydrolysis.[29] To obtain 1,10-decanedithiol, a mixture of 2.1 g (7 mmol) of 1,10-dibromodecane, 1.1 g (14 mmol) of thiourea, and 80 mL of 99.9% ethanol was refluxed under Ar atmosphere for 18 h. Following the removal of solvent under a vacuum, a solution of 0.8 g (20 mmol) of sodium hydroxide in 80 mL of water was added, and the mixture was further refluxed under Ar atmosphere for 2 h. The solution was cooled to room temperature and extracted with three 50-mL portions of diethyl ether. The combined extracts were dried over anhydrous $MgSO_4$. The ether was removed under vacuum, and the crude product was recrystallized twice from 99.9% ethanol to yield a white solid. ^{1}H NMR (500 MHz) $CDCl_3$ (ppm): 2.52 (4H, m), 1.61 (4H, m), 1.34 (2H, t), 1.22−1.32 (12H, broad). EI MS: $m/z = 206$ (M^+). 1,12-Dodecanedithiol was prepared using the same procedure as for 1,10-decanedithiol but with 1,12-dibromododecane as the starting reagent. ^{1}H NMR (500 MHz) $CDCl_3$ (ppm): 2.52 (4H, m), 1.59 (4H, m), 1.34 (2H, t), 1.26−1.30 (16H, broad). EI MS: $m/z = 234$ (M^+).

Gold substrates (Arrandee) were flame annealed before the deposition of the monolayer. This treatment leads to the formation of atomically flat Au(111) terraces.[30] Self-assembly of alkanedithiols was carried out from 1 mM solutions in ethanol. The substrates were soaked for 24 h. After the deposition, the samples were rinsed with ethanol and water and then dried in an Ar stream. Dry substrates were immediately used to form molecular junctions. The monolayers of helical peptides on gold were prepared by self-assembly from 0.5 mM solutions in a water/trifluoroethanol (60/40, v/v) mixture.[27] The adsorption time was 24 h. Modified substrates were rinsed with the water/trifluoroethanol mixture and dried in an Ar stream. It should be noted that the presence of the Acm protecting group prevents the adsorption of peptides through Cys. Thus, the molecules adsorb on gold using the free thiol group at the C-terminus, i.e., at the cysteamine linker. This way, we were able to obtain a monolayer with a uniform orientation of molecules. The substrates modified with helical peptides were subjected to a Cys (Acm) deprotection procedure.[27,28] Gold samples modified with peptides containing deprotected terminal SH groups were used to form molecular junctions, or they were tested for the presence of free thiol groups in the external plane of the monolayer. The testing procedure involved soaking the samples in an aqueous solution containing gold nanoparticles with a nominal diameter of 5 nm. The incubation time was 2 h. The samples were rinsed with water, dried, and imaged using STM.

Infrared spectroscopy was performed using a Shimadzu FTIR 8400 instrument equipped with a specular reflectance accessory (SpectraTech) at an 82° angle of incidence. p-polarized light was used. Spectra were collected as 1000 averaged scans. The tilt angles of the helical peptide molecules from surface normal were determined using the absorbance intensity ratio of the amide I/amide II bands[31]

$$\frac{I_1}{I_2} = 1.5\left[\frac{(3\cos^2\gamma - 1)(3\cos^2\theta_1 - 1) + 2}{(3\cos^2\gamma - 1)(3\cos^2\theta_2 - 1) + 2}\right] \qquad (1)$$

where I_1 and I_2 represent the observed absorbances of the amide I and amide II bands, respectively; γ is the tilt angle of the helical axis from the surface normal; and θ_1 and θ_2 represent the angles between the transition moment and the helix axis. The values of θ_1 and θ_2 were taken to be 39° and 75°, respectively.[5,9]

Electrochemical desorption experiments were carried out in a three-electrode cell with Ag wire as the reference electrode and platinum foil as the counter electrode. The supporting electrolyte was 0.1 M NaOH. The measurements were performed using a CHI750B bipotentiostat. All electrochemical experiments were carried out at 25 °C. The charges associated with desorption of thiolates from the gold surface were determined from cyclic voltammetric curves using the area under the desorption peak.

In all scanning tunneling microscopy/scanning tunneling spectroscopy (STM/STS) experiments, we used a MultiMode SPM instrument working with a Nanoscope IIIa controller (Digital Instruments, Santa Barbara, CA). Some of our experiments were carried out with a low-current converter. STM and STS data were recorded under ambient conditions in air. We used Pt/Ir STM probes (Veeco) for imaging, and for the formation of molecular junctions, we used gold tips. Gold STM tips were prepared by cutting a 0.25-mm gold wire (99.99%, Aldrich). The junctions were formed by a method analogous to that described by Haiss and co-workers.[19,24] A gold STM tip was placed at a given location on the surface of the monolayer-modified sample, and the current setting determined the distance between the tip and the substrate. In the present work, the initial value of the current was in the range of 0.05−6 nA. In all cases, the current settings were chosen so as to provide contact between the tip and the molecules forming the assembly. At these conditions, it is expected that the tip interacts with the terminal

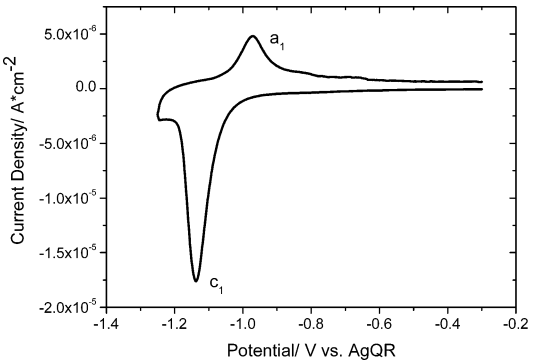

Figure 1. Cyclic voltammetric curve recorded in 0.1 M NaOH for a gold electrode modified with Acm-protected P16AA. Scan rate = 0.1 V/s.

TABLE 1: Electrochemical and FTIR-RAS Characteristics of Peptide Monolayers

	electrochemical desorption	FTIR-RAS			
SAM	$10^{10}\ \Gamma$ (mol/cm^2)	amide I position (cm^{-1})	amide II position (cm^{-1})	tilt angle (deg)	$10^{10}\ \Gamma^{\alpha}$ (mol/cm^2)
P14AA	1.12	1659	1546	43	0.79
P15AA	0.98	1661	1540	43	0.79
P16AA	1.08	1661	1545	46	0.75
P17AA	1.00	1661	1544	45	0.76

[a] A 1.4-nm diameter of the helix was assumed for the calculations. Γ denotes the surface coverage.

thiol groups of the molecules adsorbed on the substrate and Au−S bonds are formed. When the proper distance was achieved, the feedback was disabled, and the tip was lifted at a rate of 5 nm/s while keeping the $x-y$ position constant. During the vertical movement of the tip, the current was recorded as a function of the tip−sample distance. This procedure was repeated 200−300 times for each sample in order to obtain reliable statistics. We used five independently prepared samples for each monolayer. The conductance of the junctions was measured at the bias voltage of −0.4 V, which was chosen as the optimal value to achieve measurable currents for the longest molecules studied here, i.e., P16AA and P17AA.

Results and Discussion

The packing density of the monolayers formed by Acm-protected P14AA, P15AA, P16AA, and P17AA was examined by cyclic voltammetry. The surface coverage for each system was determined from reductive desorption experiments. A representative cyclic voltammogram obtained for a P16AA monolayer is shown in Figure 1. Peak c_1 observed at the cathodic part of the curve corresponds to the reductive desorption of the molecules from the gold surface, whereas anodic peak a_1 corresponds to subsequent oxidative adsorption. If we assume one-electron reduction, the charge associated with the desorption process can be easily converted to the surface coverage of the molecules immobilized on the gold surface.[32] The results obtained for peptide monolayers are reported in Table 1. It is evident that the packing densities for all peptide monolayers are similar, which is reasonable because the P14AA, P15AA, P16AA, and P17AA molecules differ only in length, whereas the cross-sectional area of the molecules remains unchanged. Assuming a 1.4-nm diameter of the helices, we concluded that the molecules are relatively densely packed within the monolayer assembly. This observation is important because the peptides were immobilized from water/TFE (60/40 v/v) solution, which has a pH of about 4.5. This means that free amino groups at the cysteine-terminal residues of the peptides are charged at these conditions, and one could expect repulsive interactions between the molecules adsorbed on the gold surface. The presence of repulsive interactions usually leads to low surface coverage, but in our case, such an effect was not observed. This can be explained by the dielectric screening of the charge localized on the free amino groups. The charges embedded in a dielectric medium, such as the water/TFE solution, interact with reduced strength because of the polarization of the molecules of solvent. Moreover, the large diameter of the helix is probably also conducive to the reduction of the strength of the electrostatic interactions because of the significant distance between neighboring molecules within the layer (at least 1.4 nm). During the self-assembly process, the peptide molecules are probably adsorbed with a proper orientation to minimize the repulsive interactions. On the other hand, the values listed in Table 1 should be considered carefully, because the packing densities obtained from electrochemical desorption experiments are usually overestimated.[33,34] This is related to the fact that the double-layer charging current can contribute significantly to the desorption charge. As a result, the value of the surface coverage calculated from the area of the desorption peak on the voltammogram can be up to 30% higher than the real value.[33,24]

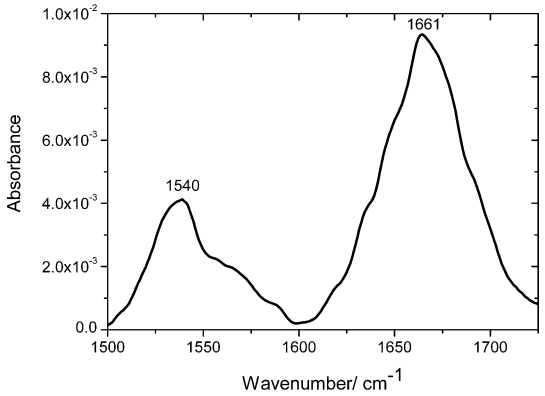

Figure 2. Amide region of the FTIR-RAS spectrum recorded for a gold substrate modified with Acm-protected P15AA.

Another approach to estimate the surface coverage is based on FTIR-RAS measurements, which also provide important information about the orientation of the molecules on the surface and the conformation of the peptide chains. A representative FTIR-RAS spectrum of P15AA is shown in Figure 2. The results obtained for all peptides are reported in Table 1. The positions of the amide I and amide II bands are indicative of the secondary structure of the peptides.[5,9,12,35] In all cases, the amide I and amide II bands appeared at the regions corresponding to an α-helical conformation of the peptide chain.[35] This confirms that the secondary structure of the peptides is preserved during the self-assembly process. Using the ratio of intensities of these two bands, we calculated the tilt angles of the helices from the surface normal (Table 1). In these calculations, we assumed a uniform orientation of the helix axis about the surface normal.[5,9,12,31] The results indicate that the peptides are not lying flat on the surface. On the basis of the tilt angles obtained from FTIR-RAS experiments, we were able to estimate the surface coverages for the peptide monolayers (see Table 1).[36] Upon comparison of these values with the results of the electrochemical desorption experiments, it is evident that the differences in coverage are in the range of 20−30%. These differences might reflect the influence of the additional charge measured in

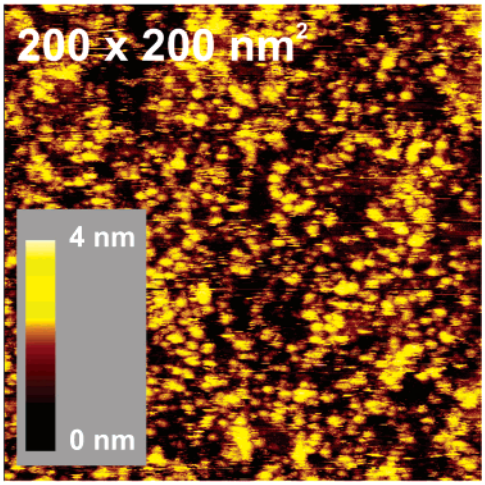

Figure 3. STM image obtained for P15AA-modified substrate after the deprotection procedure and subsequent immersion in an aqueous suspension of gold nanoparticles with a nominal diameter of 5 nm. Bias voltage = 1.2 V, tunneling current = 0.5 pA.

electrochemical desorption experiments. On the other hand, these two approaches might lead to slightly different results. The surface coverage obtained from FTIR-RAS measurements was estimated on the basis of projected molecular area, which is sensitive to the tilt angle, whereas in the case of reductive desorption, we obtained information about the number of the molecules adsorbed on the surface, which actually depends on the spacing between them. Thus, the surface coverages obtained from these two experiments might not be equivalent. Nevertheless, the results collected in Table 1 indicate that the molecules within the monolayer assemblies are relatively densely packed and the peptides adopt an α-helical conformation.

To demonstrate our ability to control the orientation of the peptide molecules adsorbed on the gold surface, we treated the monolayer assemblies with a suspension of colloidal gold. Substrates modified with monolayers of peptides containing deprotected terminal SH groups were soaked in an aqueous suspension of gold nanoparticles with a nominal diameter of 5 nm. Then, the substrates were rinsed with water, dried, and studied using STM. Figure 3 presents a typical image obtained for a P15AA monolayer. We observed a large number of gold nanoparticles immobilized on the monolayer surface. Gold colloids were strongly bonded to the top of the monolayer because their location on the surface remained unchanged during repetitive scans even under conditions where the tip occasionally touched the particle layer. This suggests that the deprotection procedure is quite effective and, as a result, free thiol groups are present in the external plane of the monolayer assembly. Strong interactions between free external thiol groups and gold colloids lead to the formation of a stable particle layer on the top of the peptide assembly. A similar testing procedure was applied for assemblies of Acm-protected peptides, but in this case, the results were negative, i.e., we did not detect gold nanoparticles immobilized on the top of the monolayers. Thus, we concluded that Acm-protected thiol groups were not available for adsorption. These observations strongly support our assumption about the uniform orientation of peptide molecules forming the monolayer, i.e., that the peptides are oriented with the C-terminus located near the gold surface and the N-terminus located in the external plane of the monolayer. It is noteworthy that the results of the testing procedure applied for monolayers of Acm-protected peptides also have further implications. Recently, Venkataraman and co-workers reported successful conductance measurements for amine-terminated molecules

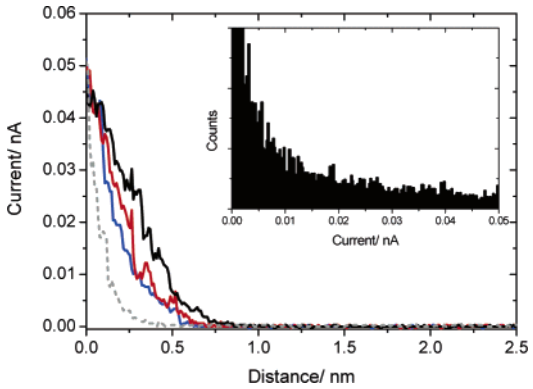

Figure 4. Examples of current−distance curves (solid lines) recorded for the molecular junctions incorporating Acm-protected P15AA. The gray dotted curve was recorded with a bare gold substrate. The inset shows the histogram for the current values obtained for the junctions incorporating Acm-protected P15AA. Bias voltage = −0.4 V.

trapped between two Au contacts.[37] Their results indicate that amines can bind to undercoordinated Au atoms in the junctions. Such binding would also be the case in our junctions because each peptide studied here has free amino groups at the cysteine residue. The cysteine unit is located in the external part of the monolayer assembly, so the amino group would be readily accessed by the STM tip. Therefore, the negative results of the testing procedure for the monolayers of Acm-protected peptides provide some important information about our systems. It seems that the interactions between the cysteine amino groups and gold are negligible in our case. Probably, this is related to the fact that the amino groups are not directly exposed on the top of the monolayer and, as a result, the interactions are minimized. To check the possibility of amine−Au binding, we also performed junction experiments with the monolayers of Acm-protected peptides. Representative current−distance curves obtained for Acm-protected P15AA are shown in Figure 4. In the course of junction formation, the STM tip might partially penetrate the monolayer, and it might also force the molecules to tilt. At these conditions, the probability of bringing the apex of the tip into contact with the amino group of cysteine is significantly higher than for the testing procedure that involved adsorption of gold colloid. If binding between the gold tip and the amino group takes place, we should record current−distance curves with well-defined current steps (current plateaus). Such current transients are indicative of electron transmission through molecules bridging the substrate and the tip.[18,19] Nevertheless, we did not observe well-defined current steps for Acm-protected peptides. The inset in Figure 4 shows a histogram that represents the frequency of the occurrence of the current values in the range between 0 and 0.05 nA. It is evident that there is no particular current value that can be distinguished in our histogram. In our opinion, the negative result of this experiment suggests that the preferred orientation of the free amino group at the terminal cysteine residue is not appropriate for direct contact with the STM tip. On the basis of the experiments described above, we concluded that, in our systems, gold−amine binding should not be competitive with gold−sulfur bonding during junction formation. The results of the experiments with the junctions based on Acm-protected peptides also verify that the Acm group successfully prevents the adsorption of the terminal sulfur atom on gold.

Figure 5 shows representative current−distance curves obtained from junction experiments using bare gold substrates (gray dashed curves) and substrates modified with deprotected peptides P15AA and P16AA (black solid curves). Each curve

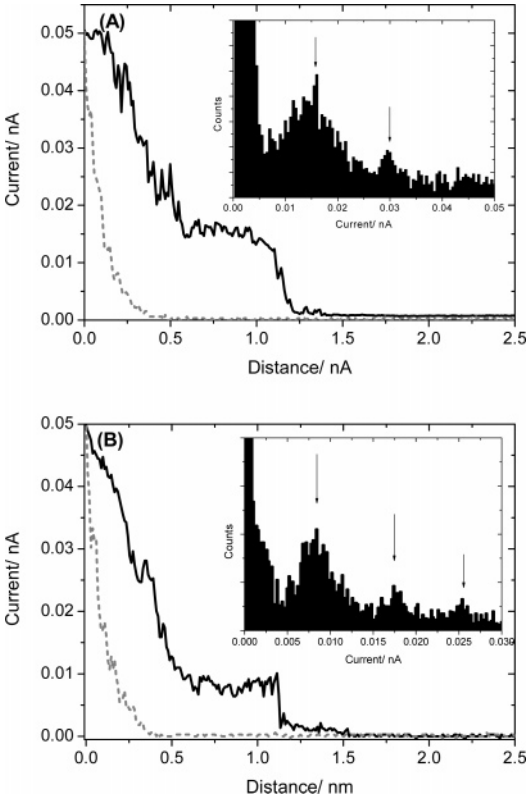

Figure 5. Representative current−distance curves obtained in individual experiments for the molecular junctions incorporating deprotected peptides (A) P15AA and (B) P16AA. The gray dashed curves were recorded using bare gold substrates. The insets show the histograms constructed on the basis of current−distance curves recorded for deprotected peptides. Bias voltage = −0.4 V.

was recorded in a single experiment at bias voltage of −0.4 V. The gray dashed curves display a rapid exponential decay of the current with increasing distance between the tip and the substrate. Such current transient is typical for electron tunneling between the tip and the bare gold. The solid black curves recorded for peptide-modified samples exhibit different characteristics. The current decays with increasing distance between the tip and the substrate, and then, the current plateau appears, which is related to the conduction through the molecule or molecules trapped between the tip and the substrate.[18,19] The current remains constant as long as the molecule is bonded to the metallic contacts, but when the contact is broken, the current drops suddenly, reflecting the low conductivity of the gap. The insets in Figure 5 show the histograms obtained from current−distance curves recorded for deprotected peptides. It should be noted that the histograms were constructed using only those curves that displayed well-defined current plateaus. In the case of the peptides, the percentage of the curves with well-defined current steps was in the range of 30−39%. All histograms shown in Figure 5 display peaks corresponding to the values of the current that appear most frequently in the current−distance curves. Therefore, the maxima are located at the values corresponding to the current plateaus. The consecutive peaks on each histogram can be ascribed to the conductance through one, two, or three molecules trapped within the junction. For further analysis, we used the current values corresponding to the first peak in the histogram, i.e., the value ascribed to the conductance of a single molecule bridging the tip and the substrate. Comparing the histograms obtained for a series of peptides, we found that the current flowing through the junction decreases in the following order: P14AA > P15AA > P16AA > P17AA. This result is reasonable if we consider that the peptides differ in length. Therefore, it can be expected that the current will decrease with increasing length of the molecules. Our data indicate that α-helical peptides obey this trend. However, the magnitude of the current decrease expressed as a decay factor (β) can be meaningful if we consider the detailed mechanism of electron transfer through these molecules. According to the model described by Petrov et al., peptide-mediated electron transfer follows a biexponential distance dependence.[4] This is related to the fact that the superexchange mechanism dominates for short-chain bridges, whereas for the longer bridges, the hopping mechanism becomes dominant. Because the superexchange and hopping mechanisms follow different distance laws, the length dependence for short peptides should follow an exponential law according to coherent tunneling, whereas for the long peptides, the distance dependence is expected to be very weak, which is typical for inelastic hopping. The experimental confirmation of this model was reported by Isied and co-workers using photolysis and radiolysis techniques.[6] These authors observed a biexponential distance dependence for the series of oligoprolines. The decay factor for short peptides was 1.4 Å^{-1}, whereas for bridges longer than 20 Å, they obtained $\beta = 0.18$ Å^{-1}. In the latter case, the contribution of the hopping mechanism to the overall electron transfer is believed to be significant. In our work, relatively long peptides containing 14−17 amino acid residues were used. The lengths of the molecules calculated as a distance between the terminal sulfur atoms are in the range of 25.0−29.5 Å.[38] Thus, we would expect that the distance dependence for our systems should also be very weak. Such an assumption is reasonable if we take into consideration the results of electrochemical investigations of electron transfer through α-helical peptides.[5,9,12] In these studies, relatively fast electron transfer was attributed to the strong contribution of the hopping mechanism. Nevertheless, the distance dependence obtained from our present measurements follows the exponential law attributed to the superexchange mechanism, and the decay constant (β) determined from the slope of the logarithmic plot of the current versus the length of the peptide was 0.50 ± 0.02 Å^{-1} (see Figure 6). In our opinion, this indicates that the dominance of the hopping mechanism in the case of α-helical peptides is not obvious. The decay factor of 0.50 Å^{-1} rather suggests that the superexchange mechanism makes a major contribution to the overall electron transfer through the α-helix and that efficient electron transmission results from the relatively low barrier for tunneling. One should take into account that the hydrogen bonds present in the helical

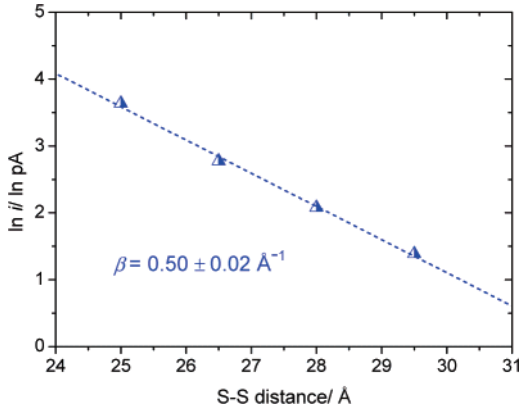

Figure 6. Logarithmic plot of the current as a function of the peptide length. The length corresponds to the distance between terminal sulfur atoms. The value of the decay constant (β) was obtained from the slope of this plot.

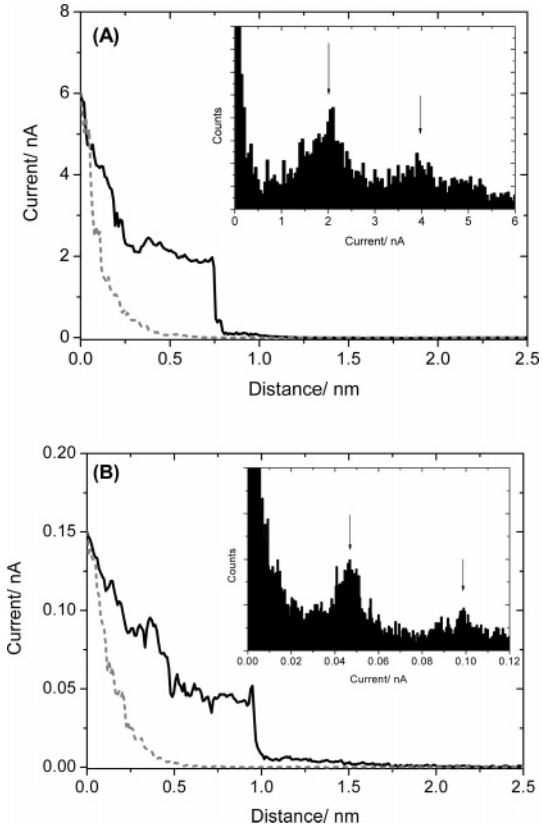

Figure 7. Examples of the current−distance curves recorded in individual experiments for the molecular junctions incorporating alkanedithiols (A) 1,8-octanedithiol and (B) 1,12-dodecanedithiol. The gray dashed curves were recorded using bare gold substrates. The insets show the histograms constructed on the basis of current−distance curves recorded for alkanedithiols. Bias voltage = −0.4V.

structure can influence the barrier height.[8,16] Moreover, the efficiency of electron transfer mediated by hydrogen bonds is similar to that observed for covalent bonds.[39] Thus, the presence of hydrogen bonds might lead to shortening of the electron-transfer pathway through the α-helix. Of course, more objective conclusions can be made if the value of the decay factor obtained from our experiments is referred to well-known systems. To check the validity of our explanation, we performed a series of experiments with alkanedithiols. We chose these compounds because electron transfer mediated by simple *n*-alkyl bridges is widely described in the literature.[18,19,40−42] All measurements were carried out at exactly the same conditions as for peptides. The molecular junctions were formed with 1,8-octanedithiol, 1,9-nonanedithiol, 1,10-decanedithiol, and 1,12-dodecanedithiol. Figure 7 shows representative current−distance curves obtained for the junctions incorporating 1,8-octanedithiol and 1,12-dodecanedithiol. The histograms were constructed using the curves displaying well-defined current steps. The percentage of current−distance curves with well-defined plateaus obtained for alkyldithiols was in the range of 28−40%. The consecutive maxima on each histogram were ascribed to conductance through one or two molecules bridged between the tip and the substrate. As previously, for further analysis, we used the currents corresponding to the conductances of single molecules. Figure 8 presents a logarithmic plot of the current versus the length of the molecules. The currents measured for alkanedithiols are plotted together with the data obtained for peptides. The lengths of the alkanedithiols were calculated as the distances between terminal sulfur atoms assuming an all-trans conformation of the alkyl chains.[38] The distance dependence for alkanedithiols is exponential, as expected for a coherent electron tunneling process. We found that the decay factor was 0.75 ± 0.03 $Å^{-1}$, which corresponds to 0.94 per CH_2 group. This value is reasonable, because the decay factors obtained from various junction experiments with *n*-alkyl bridges usually range between 0.8 and 1.2 per methylene unit.[18,42−46]

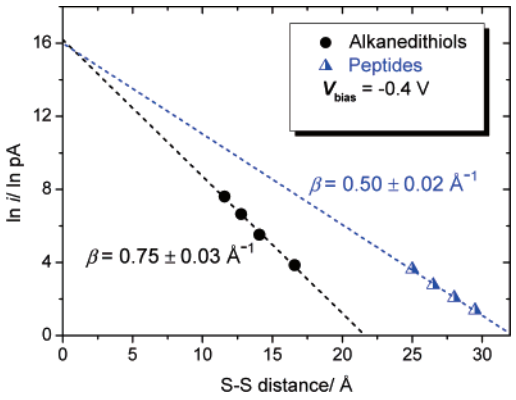

Figure 8. Logarithmic plot of the current as a function of the length of the molecules trapped within the junction. The lengths of the molecules were calculated as distances between terminal sulfur atoms. The data obtained for alkanedithiols (circles) and peptides (triangles) are plotted together for comparison.

A direct comparison of the data obtained for alkanedithiols and peptides shows that the decay factor for electron transmission through an α-helix is reduced by ca. 30%. Therefore, our assumption of a coherent tunneling mechanism for electron transfer through helical peptides is correct. A Strong contribution of hopping should result in a significantly lower decay factor as discussed above. It is also interesting that the logarithmic plots of current versus length for peptides and alkyldithiols intercept the ordinate axis at similar values, which means that there is a small difference in the prefactors of the exponential functions for alkyl and peptide bridges. This might suggest that, for α-helical peptides shorter than 29.5 Å, there is no inflection point in the distance dependence. Such an inflection would be expected if a transition between the superexchange and hopping mechanisms takes place.

We realize that the STM-based molecular junction method used in this work has some disadvantages because distortion of the secondary structure of the helix during the conductivity measurement cannot be excluded. At the initial stage of junction formation, the distance between the tip and the substrate is smaller than the monolayer thickness, and a possible scenario assumes that, during tip approach, the molecule trapped within the junction is forced to tilt. Further, the tip is moved upward, and the molecule is lifted. At this stage, the helical conformation of the molecule is probably unchanged. Thus, the current results from electron transfer through the helix. The question is whether the current drop observed in the STS experiments is related to the breakage of the Au−S linkage or is caused by the conformational transition of the helix due to the vertical movement of the tip. This issue is quite problematic. It should be noted that conformational change from a helical to a fully extended structure must involve the disruption of hydrogen bonds and salt bridges and changes in torsion angles within the peptide. This might be unfavorable for the unfolding of the peptide backbone. However, if we assume that conformational changes occur, we should consider the resulting expected difference in conductance. This difference is probably significant, i.e., the conductance of the fully extended structure might be much lower than that of the α-helix. This is reasonable if we compare the lengths of the same peptide with helical and fully

extended conformations. For example, if we consider the P14AA molecule, the distance between terminal sulfur atoms is ca. 2.5 nm, whereas in the second case, this distance should be about 5.5 nm. This suggests that the structural transition should lead to a significant decrease of the conductance because of the substantial change in the length of the electron-transfer pathway. As a result, the current related to electron transfer through extended structure might be very low. Finally, the sudden drop of the current observed during the STS experiments might reflect the disruption of Au−S bonds as well as the structural transition of the peptide from a helix to some extended conformation. Of course, the change of the secondary structure of the peptide might involve some intermediate structures, with conductances between those corresponding to helical and extended conformations. Thus, we could expect sequential changes in conductance, and hence, the current measured in the STS experiments should change in a similar manner. This scenario seems to be probable, but we should also consider the time scale of the conformational transition. It is highly likely that the conformational transition is very fast (e.g., in the nanosecond range);[47] thus, we are not able to observe a sequential change of the conductance because of the relatively large time scale of our experiments. Nevertheless, in some cases, we observed that the current recorded during the STS experiments drops to nonzero values after the current step (see curve B in Figure 5). This weak current might correspond to low-conductive conformations of the stretched peptide backbone. On the other hand, nonzero currents following the current step were also observed for some molecular junctions incorporating alkanedithiols (see Figure 7). Thus, the origin of these weak currents might be completely different. For example, it might result from weak interactions (i.e., physical adsorption) between the tip and the molecules.[48]

Summary

We have demonstrated the ability to control the orientation of thio-modified α-helical peptides adsorbed on a gold surface. Using the molecular junction approach, we determined the electron-transfer efficiencies of a series of synthetic peptides. Comparison of the conductances of α-helical bridges with simple *n*-alkyl spacers shows that the superexchange mechanism makes a major contribution to the overall electron transfer mediated by an α-helical structure. Efficient electron transmission can be related to a low barrier for tunneling as indicated by the value of the decay constant equal to 0.50 $Å^{-1}$.

Acknowledgment. This work was supported by KBN, Grant 3 T09A 01627, and MENiS funds, Project 120000-501/68-BW-1681/15/05. We thank Dr. Barbara Palys for FTIR-RAS measurements.

References and Notes

(1) Marcus, R. A.; Sutin, N. *Biochim. Biophys. Acta* **1985**, *811*, 265.
(2) Wasielewski, M. R. *Chem. Rev.* **1992**, *92*, 435.
(3) Isied, S. S.; Ogawa, M. Y.; Wishart, J. F. *Chem. Rev.* **1992**, *92*, 381.
(4) Petrov, E. G.; Shevchenko, Y. V.; Teslenko, V. I.; May, V. *J. Chem. Phys.* **2001**, *115*, 7107.
(5) Morita, T.; Kimura, S. *J. Am. Chem. Soc.* **2003**, *125*, 8732.
(6) Malak, R. A.; Gao, Z.; Wishart, J. F.; Isied, S. S. *J. Am. Chem. Soc.* **2004**, *126*, 13888.
(7) Sek, S.; Sepiol, A.; Tolak, A.; Misicka, A.; Bilewicz, R. *J. Phys. Chem. B* **2004**, *108*, 8102.
(8) Polo, F.; Antonello, S.; Formaggio, F.; Toniolo, C.; Maran, F. *J. Am. Chem. Soc.* **2005**, *127*, 492.
(9) Watanabe, J.; Morita, T.; Kimura, S. *J. Phys. Chem. B* **2005**, *109*, 14416.
(10) Long, Y.-T.; Abu-Irhayem, E.; Kraatz, H. B. *Chem. Eur. J.* **2005**, *11*, 5186.
(11) Joachim, C.; Ratner, M. A. *Proc. Natl. Acad. Sci. U.S.A.* **2005**, *102*, 8801.
(12) Sek, S.; Tolak, A.; Misicka, A.; Palys, B.; Bilewicz, R. *J. Phys. Chem. B* **2005**, *109*, 18433.
(13) Shin, Y. K.; Newton, M. D.; Isied, S. S. *J. Am. Chem. Soc.* **2003**, *125*, 3722.
(14) Sisido, M.; Hoshino, S.; Kusano, H.; Kuragaki, M.; Makino, M.; Sasaki, H.; Smith, T. A.; Ghiggino, K. P. *J. Phys. Chem. B* **2001**, *105*, 10407.
(15) Sasaki, H.; Makino, M.; Sisido, M.; Smith, T. A.; Ghiggino, K. P. *J. Phys. Chem. B* **2001**, *105*, 10416.
(16) Antonello, S.; Formaggio, F.; Moretto, A.; Toniolo, C.; Maran, F. *J. Am. Chem. Soc.* **2003**, *125*, 2874.
(17) Kraatz, H. B.; Bediako-Amoa, I.; Gyepi-Garbrah, S. H.; Sutherland, T. C. *J. Phys. Chem. B* **2004**, *108*, 20164.
(18) Xu, B.; Tao, N. J. *Science* **2003**, *301*, 1221.
(19) Haiss, W.; Nichols, R. J.; van Zalinge, H.; Higgins, S. J.; Bethell, D.; Schiffrin, D. J. *Phys. Chem. Chem. Phys.* **2004**, *6*, 4330.
(20) He, J.; Chen, F.; Li, J.; Sankey, O. F.; Terazono, Y.; Herrero, C.; Gust, D.; Moore, T. A.; Moore, A. L.; Lindsay, S. M. *J. Am. Chem. Soc.* **2005**, *127*, 1384.
(21) Xu, B. Q.; Zhang, P. M.; Li, X. L.; Tao, N. J. *Nano Lett.* **2004**, *4*, 1105.
(22) Hihath, J.; Xu, B. Q.; Zhang, P. M.; Tao, N. J. *Proc. Natl. Acad. Sci. U.S.A.* **2005**, *102*, 16979.
(23) Wierzbinski, E.; Arndt, J.; Hammond, W.; Slowinski, K. *Langmuir* **2006**, *22*, 2426.
(24) Haiss, W.; van Zalinge, H.; Higgins, S. J.; Bethell, D.; Hobenreich, H.; Schiffrin, D. J.; Nichols, R. J. *J. Am. Chem. Soc.* **2003**, *125*, 15294.
(25) Xiao, X. Y.; Xu, B. Q.; Tao, N. J. *J. Am. Chem. Soc.* **2004**, *126*, 5370.
(26) Xiao, X.; Xu, B.; Tao, N. *Angew. Chem., Int. Ed.* **2004**, *43*, 6148.
(27) Sek, S.; Swiatek, K.; Misicka, A. *J. Phys. Chem. B* **2005**, *109*, 23121.
(28) Veber, D. F.; Milkowski, J. D.; Varga, S. L.; Denkewalter, R. G.; Hirschmann, R. *J. Am. Chem. Soc.* **1972**, *94*, 5456.
(29) Witt, D.; Klajn, R.; Barski, P.; Grzybowski, B. A. *Curr. Org. Chem.* **2004**, *8*, 1763.
(30) Haiss, W.; Lackey, D.; Sass, J. K.; Besocke, K. H. *J. Chem. Phys.* **1991**, *95*, 2193.
(31) Gremlich, H. U.; Frigeli, U. P.; Schwyzer, R. *Biochemistry* **1983**, *22*, 4257.
(32) Walczak, M. M.; Popenoe, D. D.; Deinhammer, R. S.; Lamp, B. D.; Chung, C.; Porter, M. D. *Langmuir* **1991**, *7*, 2687.
(33) Schneider, T. W.; Buttry, D. A. *J. Am. Chem. Soc.* **1993**, *115*, 12391.
(34) Kakiuchi, T.; Usui, H.; Hobara, D.; Yamamoto, M. *Langmuir* **2002**, *18*, 5231.
(35) Kennedy, D. F.; Crisma, M.; Toniolo, C.; Chapman, D. *Biochemistry* **1991**, *30*, 6541.
(36) Bin, X.; Zawisza, I.; Goddard, J. D.; Lipkowski, J. *Langmuir* **2005**, *21*, 330.
(37) Venkataraman, L.; Klare, J. E.; Tam, I. W.; Nuckolls, C.; Hybertsen, M. S.; Steigerwald, M. L. *Nano Lett.* **2006**, *6*, 458.
(38) The distance between the terminal sulfur atoms was calculated using HyperChem 6.0. It was assumed that the peptides adopt a helical structure with dihedral angles $\omega = 180°$, $\phi = -58°$, and $\psi = -47°$. In the case of alkanedithiols, ae assumed an all-trans conformation of alkyl chain, and the bond lengths (in Å) used in these calculations were S−C = 1.79 and C−C = 1.54.
(39) de Rege, P. J. F.; Wiliams, S. A.; Therien, M. J. *Science* **1995**, *269*, 1409.
(40) Wold, D. J.; Frisbie, C. D. *J. Am. Chem. Soc.* **2000**, *122*, 2970.
(41) Cui, X. D.; Primak, A.; Zarate, X.; Tomfohr, J.; Sankey, O. F.; Moore, A. L.; Moore, T. A.; Gust, D.; Harris, G.; Lindsay, S. M. *Science* **2001**, *294*, 571.
(42) Wold, D. J.; Haag, R.; Rampi, M. A.; Frisbie, C. D. *J. Phys. Chem. B* **2002**, *106*, 2813.
(43) Slowinski, K.; Fong, H. K. Y.; Majda, M. *J. Am. Chem. Soc.* **1999**, *121*, 7257.
(44) York, R. L.; Nguyen, P. T.; Slowinski, K. *J. Am. Chem. Soc.* **2003**, *125*, 5948.
(45) Sek, S.; Bilewicz, R.; Slowinski, K. *Chem. Commun.* **2004**, 404.
(46) Li, X.; He, J.; Hihath, J.; Xu, B.; Lindsay, S. M.; Tao, N. *J. Am. Chem. Soc.* **2006**, *128*, 2135.
(47) Brooks, C. L., III. *J. Phys. Chem.* **1996**, *100*, 2546.
(48) Wierzbinski, E.; Slowinski, K. *Langmuir* **2006**, *22*, 5205.